Journal of Nuclear Materials 407 (2010) 110–115

Contents lists available at ScienceDirect

Journal of Nuclear Materials

journal homepage: www.elsevier.com/locate/jnucmat

Comparison of some lead and non-lead based glass systems, standard shielding concretes and commercial window glasses in terms of shielding parameters in the energy region of 1 keV–100 GeV: A comparative study

Murat Kurudirek [a,*], Yüksel Özdemir [a], Önder Şimşek [b], Rıdvan Durak [a]

[a] *Faculty of Science, Department of Physics, Ataturk University, 25240 Erzurum, Turkey*
[b] *Faculty of Education, Department of Physics Education, Ataturk University, 25240 Erzurum, Turkey*

ARTICLE INFO

Article history:
Received 18 July 2010
Accepted 6 October 2010

ABSTRACT

The effective atomic numbers, Z_{eff} of some glass systems with and without Pb have been calculated in the energy region of 1 keV–100 GeV including the *K* absorption edges of high *Z* elements present in the glass. Also, these glass systems have been compared with some standard shielding concretes and commercial window glasses in terms of mean free paths and total mass attenuation coefficients in the continuous energy range. Comparisons with experiments were also provided wherever possible for glasses. It has been observed that the glass systems without Pb have higher values of Z_{eff} than that of Pb based glasses at some high energy regions even if they have lower mean atomic numbers than Pb based glasses. When compared with some standard shielding concretes and commercial window glasses, generally it has been shown that the given glass systems have superior properties than concretes and window glasses with respect to the radiation-shielding properties, thus confirming the availability of using these glasses as substitutes for some shielding concretes and commercial window glasses to improve radiation-shielding properties in the continuous energy region.

1. Introduction

By the extensive use of nuclear energy and radioactive isotopes in various fields' viz. reactors, nuclear power plants, nuclear engineering and space technology, the radiation shielding became an important subject due to required proper precautions to avoid from the radiation hazards. For the shielding purposes, the glass systems have double functions of being transparent to visible light and absorbing gamma rays and neutrons, thus providing a radiation shield for observers and experimenters [1]. Effective atomic number which is representing the radiation attenuation in the absorbing medium is related to the radiation interaction with matter and is useful in some applications such as designing radiation shielding, computing absorbed dose and buildup factor [2]. The effective atomic number is similar to that atomic number of elements [3]. However, on the basis of Hine's expression [4] that the effective atomic number of a material composed of several elements can not be expressed by a single number, it can be concluded that it is an energy dependent parameter due to the different partial photon interaction processes with matter for which the various atomic numbers in the material have to be weighted differently. Studies on radiation-shielding properties of different types of glasses have been made before for some photon energies [5–10], but studies regarding continuous energy region (i.e. 1 keV–100 GeV) are very scarce [1]. Comparison of glass systems with shielding concretes has been done by a limited number of concretes and most of them appear to be restricted to a limited energy range. Looking from these aspects, the present study aimed at (a) investigation and comparison of effective atomic numbers of some glass systems in the wide energy region of 1 keV–100 GeV, (b) comparison of the glass systems with seven types of concretes and two types of commercial window glasses to seek the availability of the used glass systems with respect to the radiation shielding.

2. Calculation method

The effective atomic numbers of glass systems can be calculated by the following practical formula [11]:

$$Z_{eff} = \frac{\sum_i f_i A_i (\mu/\rho)_i}{\sum_j f_j \frac{A_j}{Z_j} (\mu/\rho)_j} \qquad (1)$$

where f_i is the molar fraction, A_i is the atomic weight, Z_j is the atomic number, $(\mu/\rho)_i$ is the mass attenuation coefficient. The total mass attenuation coefficients of elements present in the glass systems have been obtained from the WinXCom [12,13] computer program.

---

* Corresponding author. Tel.: +90 442 2314167; fax: +90 442 23609 48.
E-mail address: mkurudirek@gmail.com (M. Kurudirek).

0022-3115/$ - see front matter © 2010 Elsevier B.V. All rights reserved.
doi:10.1016/j.jnucmat.2010.10.007

The mean free path (mfp) represents the average distance between two successive interactions of photons in which the intensity of incident photon beam is reduced by the factor of 1/*e*. For the detailed knowledge on calculations of the total mass attenuation coefficients and mean free paths (mfp) of the present glass systems, concretes and commercial window glasses, we may refer to a previous study [14].

3. Results and discussion

The chemical compositions of the used glasses have been given in Table 1[5–7]. Fig. 1a–c shows the variation of Z_{eff} with incident photon energy from 1 keV to 100 GeV. On the basis of the relative domination of the partial photon interaction processes, viz., photoelectric absorption, Compton scattering and pair production, the significant variations in Z_{eff} were noted. The variation in Z_{eff} is large below 100 keV where photoelectric process dominates and the variation is negligible between about 1 and 2 MeV where the Compton scattering is pre-dominating and further there is also a significant change in Z_{eff} which is due to the pair production process. It was observed that the Z_{eff} has maximum values below 100 keV and has minimum values at intermediate energies. At the corresponding *K* absorption edge of high *Z* element present in the glass, the effective atomic number can has more than a single value, thus revealing the non-availability of using Z_{eff} in this energy region. The all variations can be clearly explained by the *Z* dependence of total atomic cross sections thus effective atomic numbers as Z^{4-5} for photoelectric absorption, *Z* for Compton scattering and Z^2 for pair production.

Fig. 2a and b shows the comparison of lead free glass systems with lead based glasses according to the effective atomic numbers. We have compared the glass systems by matching the same or less weight fraction of BaO with that of PbO present in the glass samples. From the Fig. 2a it can be clearly seen that the BaO–Flyash–B_2O_3 glass has higher values of Z_{eff} than PbO–B_2O_3 glass from about 300 keV to further energies except for the 0.44BaO–0.16Flyash–0.40B_2O_3 and 0.50PbO–0.50B_2O_3 glasses for which the BaO glass has higher values of Z_{eff} than PbO glass from 500 keV to 25 MeV. According to the Fig. 2b, the BaO–P_2O_5 glass has higher values of Z_{eff} than PbO–B_2O_3 glass from 350 keV to 80 MeV for 0.30BaO–0.70P_2O_5, from 400 keV to 25 MeV for 0.40BaO–0.60P_2O_5, from 510 keV to 15 MeV for 0.50BaO–0.50P_2O_5, from 600 keV to 10 MeV for 0.60BaO–0.40P_2O_5, from 800 keV to 5 MeV for 0.70BaO–0.30P_2O_5 glass. Also, it was observed that with the increasing weight fraction of high Z element (viz. Ba, Pb) in the glass system the Z_{eff} also increases at some photon energies (Fig. 3).

Finally, we have compared the calculated Z_{eff} values with the available experimental Z_{eff} values present in the literature. From the Table 2, one can easily observe that our calculated values are in good agreement with the experimentally obtained ones within a few percent uncertainties. Table 3 lists the descriptive statistics of the calculated effective atomic numbers along with the mean atomic numbers for some glass systems.

When it comes to radiation shielding, the mean free path (mfp) which is defined as the average distance between two successive interactions of photons becomes one of the most appropriate

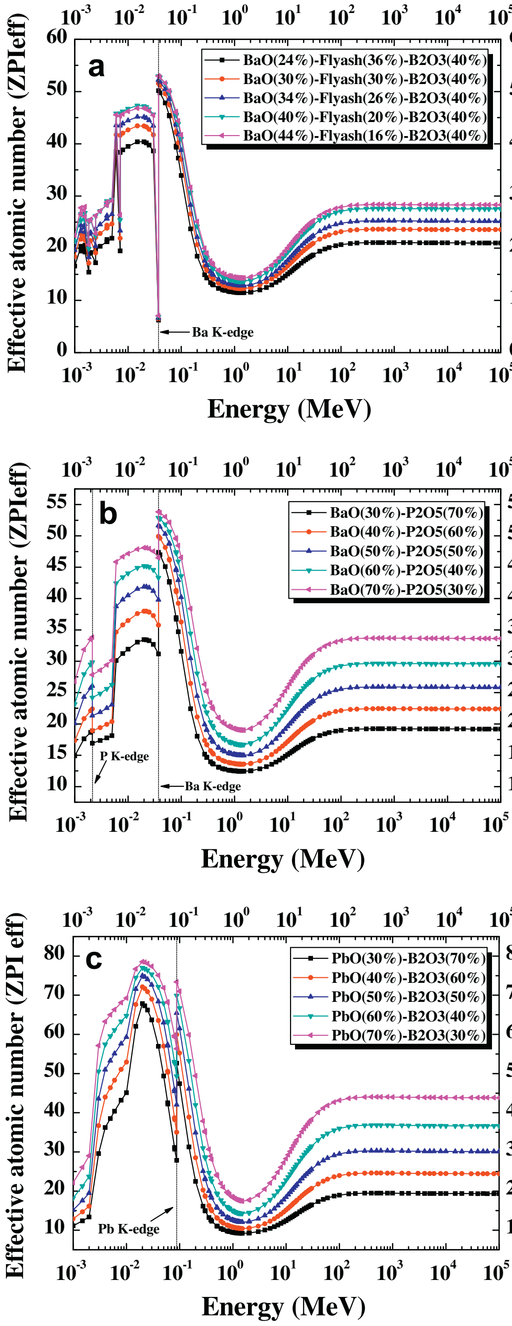

Fig. 1. (a–c) Effective atomic numbers of the given glasses for total photon interaction from 1 keV to 100 GeV.

Table 1
Chemical composition of glass samples.

Sample	Chemical composition (wt.%)		
Lead based			
	PbO	B_2O_3	
1	30	70	
2	40	60	
3	50	50	
4	60	40	
5	70	30	
Non-lead based			
	BaO	P_2O_5	
1	30	70	
2	40	60	
3	50	50	
4	60	40	
5	70	30	
	BaO	Flyash	B_2O_3
6	24	36	40
7	30	30	40
8	34	26	40
9	40	20	40
10	44	16	40

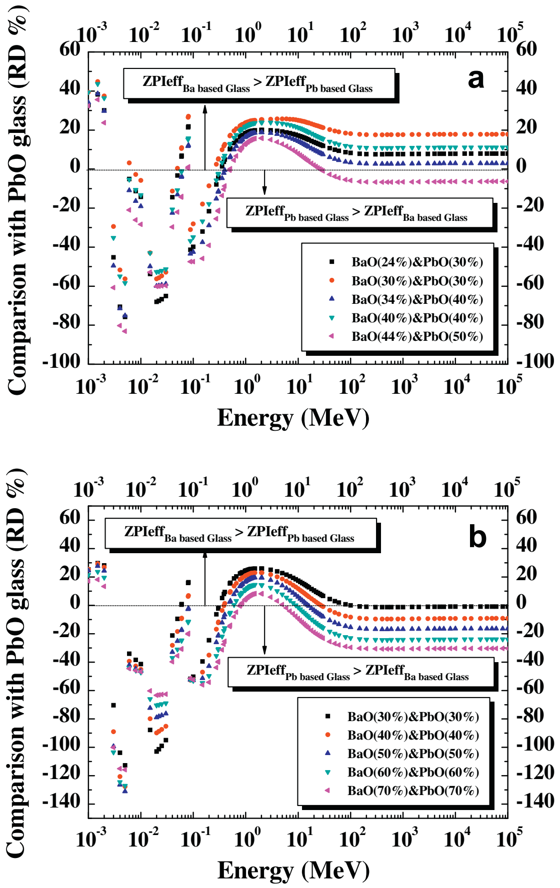

Fig. 2. (a) and (b) Differences in effective atomic numbers between lead based and non-lead based glass systems.

parameter representing the radiation attenuation. The present glass systems have been compared with some standard shielding concretes which are available in a previous study [15] in terms of mfp in the energy region of 1 keV–100 GeV (Figs. (4 and 5)). The all types of BaO–Flyash–B_2O_3 glasses have lower values of mfp than ordinary concrete from 20 keV to 100 GeV, than hematite-serpentine and basalt–magnetite concretes from 30 keV to 100 GeV. Except for the 0.24BaO–0.36Flyash–0.40B_2O_3 glass, the BaO–Flyash–B_2O_3 glasses have lower values of mfp than ilmenite–limo-

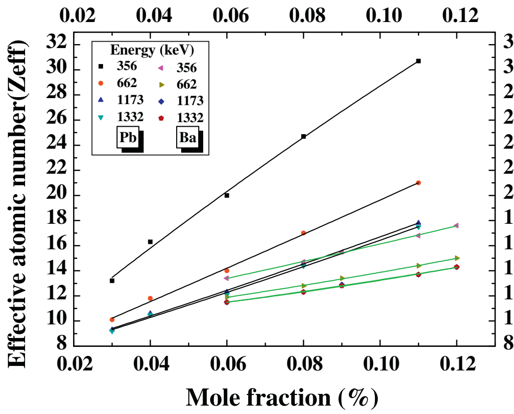

Fig. 3. Variation of effective atomic numbers with mole fractions of Pb and Ba at some photon energies.

Table 3
Descriptive statistics for calculated effective atomic numbers of given glasses along with the mean atomic numbers.

Glass systems	Z_{mean}	ZPI_{eff}	
		Min	Max
BaO–Flyash–B_2O_3[f]	14.1	6.2	50.2
BaO–Flyash–B_2O_3[g]	15.4	6.5	51.5
BaO–Flyash–B_2O_3[h]	16.3	6.6	52.2
BaO–Flyash–B_2O_3[i]	17.6	6.9	53.0
BaO–Flyash–B_2O_3[j]	18.4	7.1	53.0
BaO–P_2O_5[a]	16.6	12.4	47.4
BaO–P_2O_5[b]	18.8	13.6	49.9
BaO–P_2O_5[c]	21.0	15.0	51.7
BaO–P_2O_5[d]	23.2	16.7	52.9
BaO–P_2O_5[e]	25.4	19.0	53.8
PbO–B_2O_3[a]	18.3	9.2	67.9
PbO–B_2O_3[b]	22.1	10.5	72.1
PbO–B_2O_3[c]	25.9	12.1	75.0
PbO–B_2O_3[d]	29.7	14.3	77.0
PbO–B_2O_3[e]	33.5	17.4	78.5

[a] (x)PbO–$(100-x)B_2O_3$ where $x = 30$.
[b] (x)PbO–$(100-x)B_2O_3$ where $x = 40$.
[c] (x)PbO–$(100-x)B_2O_3$ where $x = 50$.
[d] (x)PbO–$(100-x)B_2O_3$ where $x = 60$.
[e] (x)PbO–$(100-x)B_2O_3$ where $x = 70$.
[f] (x)BaO–$(0.6-x)$Flyash–$(0.4)B_2O_3$ where $x = 0.24$.
[g] (x)BaO–$(0.6-x)$Flyash–$(0.4)B_2O_3$ where $x = 0.30$.
[h] (x)BaO–$(0.6-x)$Flyash–$(0.4)B_2O_3$ where $x = 0.34$.
[i] (x)BaO–$(0.6-x)$Flyash–$(0.4)B_2O_3$ where $x = 0.40$.
[j] (x)BaO–$(0.6-x)$Flyash–$(0.4)B_2O_3$ where $x = 0.44$.

Table 2
Experimental effective atomic numbers along with the calculated ones in the present study.

Energy (MeV)	BaO–Flyash–B_2O_3 (I)[a]		BaO–Flyash–B_2O_3 (II)[b]		BaO–Flyash–B_2O_3 (III)[c]		BaO–Flyash–B_2O_3 (IV)[d]		BaO–Flyash–B_2O_3 (V)[e]	
	Z_{eff} exp.	Z_{eff} theo.	Z_{eff} exp.	Z_{eff} theo.	Z_{eff} exp.	Z_{eff} theo.	Z_{eff} exp.	Z_{eff} theo.	Z_{eff} exp.	Z_{eff} theo.
3.56E−01	12.4[g]	13.3	13.5	14.6	14.6	15.4	16.0	16.7	17.1	17.4
6.62E−01	12.2	11.8	13.1	12.7	13.8	13.3	14.9	14.3	15.4	14.9
1.17E+00	11.8	11.5	12.5	12.3	13.0	12.8	14.0	13.7	14.6	14.3
1.33E+00	11.8	11.5	12.7	12.3	13.3	12.8	14.1	13.7	14.7	14.3
	PbO–B_2O_3 (I)[f]		PbO–B_2O_3 (II)		PbO–B_2O_3 (III)		PbO–B_2O_3 (IV)		PbO–B_2O_3 (V)	
6.62E-01	10.0[g]	10.1	12.0	11.8	13.6	14.0	16.3	17.0	21.3	21.0

[a] (x)BaO–$(0.6-x)$Flyash–$(0.4)B_2O_3$ where $x = 0.24$.
[b] (x)BaO–$(0.6-x)$Flyash–$(0.4)B_2O_3$ where $x = 0.30$.
[c] (x)BaO–$(0.6-x)$Flyash–$(0.4)B_2O_3$ where $x = 0.34$.
[d] (x)BaO–$(0.6-x)$Flyash–$(0.4)B_2O_3$ where $x = 0.40$.
[e] (x)BaO–$(0.6-x)$Flyash–$(0.4)B_2O_3$ where $x = 0.44$.
[f] (x)PbO–$(100-x)B_2O_3$ where $x = 30, 40, 50, 60, 70$, respectively.
[g] Experimentally obtained values by Singh et al. [5] and Kirdsiri et al. [6], respectively.

nite concrete from 30 keV to 100 GeV. The 0.24BaO–0.36Flyash–0.40B_2O_3 glass has lower values of mfp than ilmenite–limonite concrete from 30 to 400 keV, has about the same values with ilmenite–limonite concrete from 400 keV to 60 MeV and has slightly higher values than ilmenite–limonite concrete from 60 MeV to 100 GeV. The mfp of all types of BaO–Flyash–B_2O_3 glasses are lower than ilmenite concrete from 30 to 200 keV, from 200 keV to 100 GeV the ilmenite concrete has lower values of mfp than 0.24BaO–0.36Flyash–0.40B_2O_3, from 200 keV to 15 MeV the ilmenite concrete has also lower values of mfp than 0.3BaO–0.3Flyash–0.4B_2O_3, after 15 MeV the values of mfp become slightly higher for ilmenite concrete than 0.3BaO–0.3Flyash–0.4B_2O_3. The steel-scrap concrete has higher values of mfp than all types of glasses between 50–200 keV while it has lower values of mfp than all types of glasses from 800 keV to 10 MeV. From 10 MeV to 100 GeV only the 0.44BaO–0.16Flyash–0.40B_2O_3 glass has lower values of mfp than steel-scrap concrete. Finally, it has been observed from Fig. 4g that the steel–magnetite concrete has lower values of mfp than all types of BaO–Flyash–B_2O_3 glasses from 300 keV to 100 GeV. From the Fig. 5, it has been observed that all types of PbO–B_2O_3 glasses have lower values of mfp than ordinary, hematite-serpentine, ilmenite–limonite, basalt–magnetite and ilmenite concretes. The steel-scrap concrete has higher values of mfp than all PbO–B_2O_3 glasses from 30 to 500 keV whereas it has lower values of mfp than only 0.3PbO–0.7B_2O_3 glass from 1 MeV to 100 GeV. From 60 to 300 keV, the steel–magnetite concrete has higher values of mfp than all types of PbO–B_2O_3 glasses whereas it has lower values than the PbO–B_2O_3 glasses except for the 0.7PbO–0.3B_2O_3 glass between 1 and 4 MeV and has lower values than the PbO–B_2O_3 glasses up to the 0.6PbO–0.4B_2O_3 glasses between 1 and 10 MeV. From 10 MeV to 100 GeV the steel-magnetite concrete has lower values of mfp than the 0.3PbO–0.7B_2O_3 and 0.4PbO–0.6B_2O_3 glasses. From the Fig. 6a–c, it is seen that the total mass attenuation coefficients of PbO–B_2O_3, BaO–Flyash–B_2O_3 and BaO–P_2O_5 are higher than that of commercial window glasses [16] except for some energy regions where Compton scattering is pre-dominating. In this energy region the total mass attenuation coefficient seem to be independent of chemical composition and the values of total mass attenuation coefficients are practically the same. The energy regions where Compton scattering is predominant are 400 keV–5 MeV for BaO–Flyash–B_2O_3, 500 keV–4 MeV for BaO–P_2O_5 and 1–2 MeV for PbO–B_2O_3 glasses.

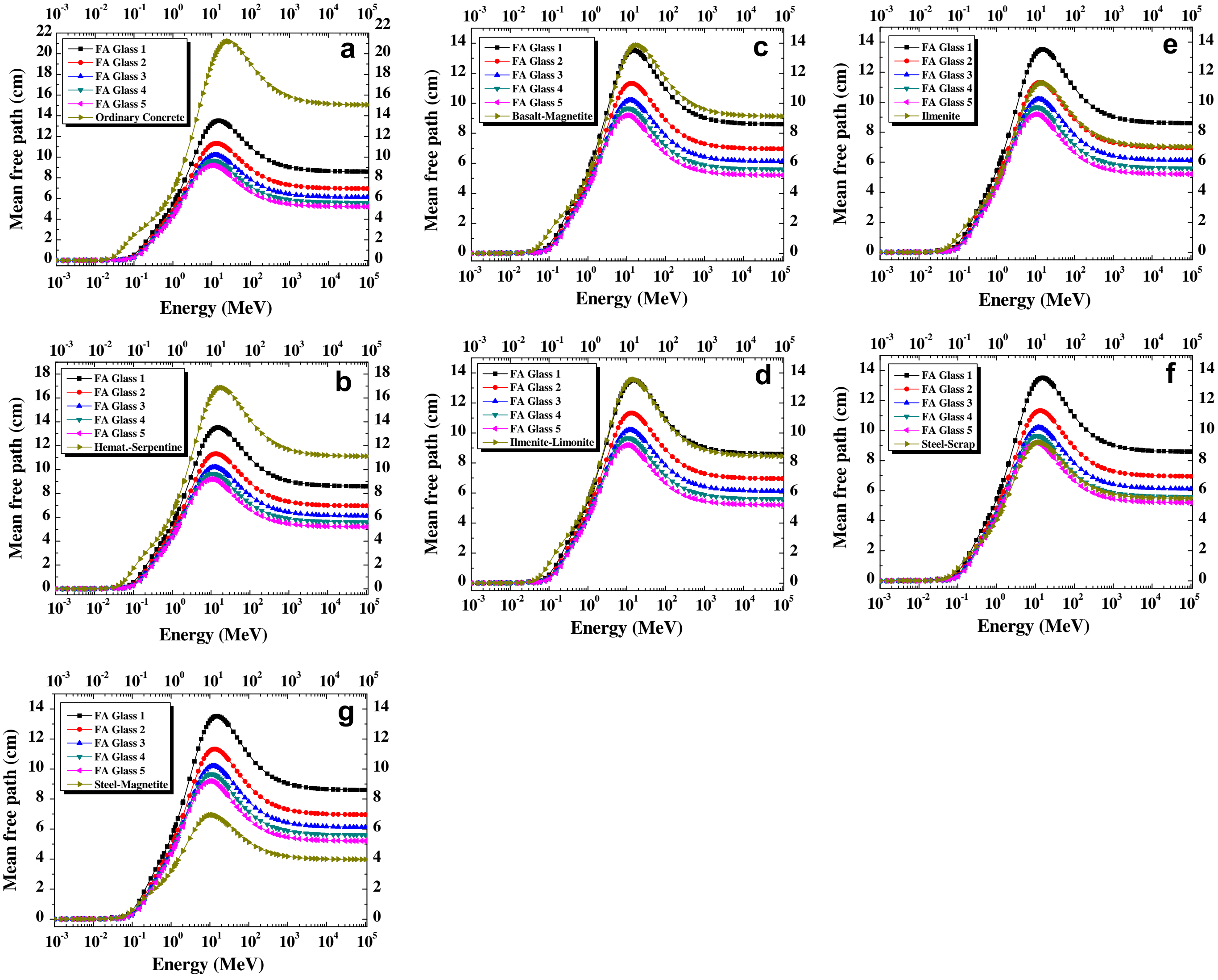

Fig. 4. (a–g) Mean free paths of BaO–Flyash–B_2O_3 glass and different types of concretes in the energy region of 1 keV–100 GeV.

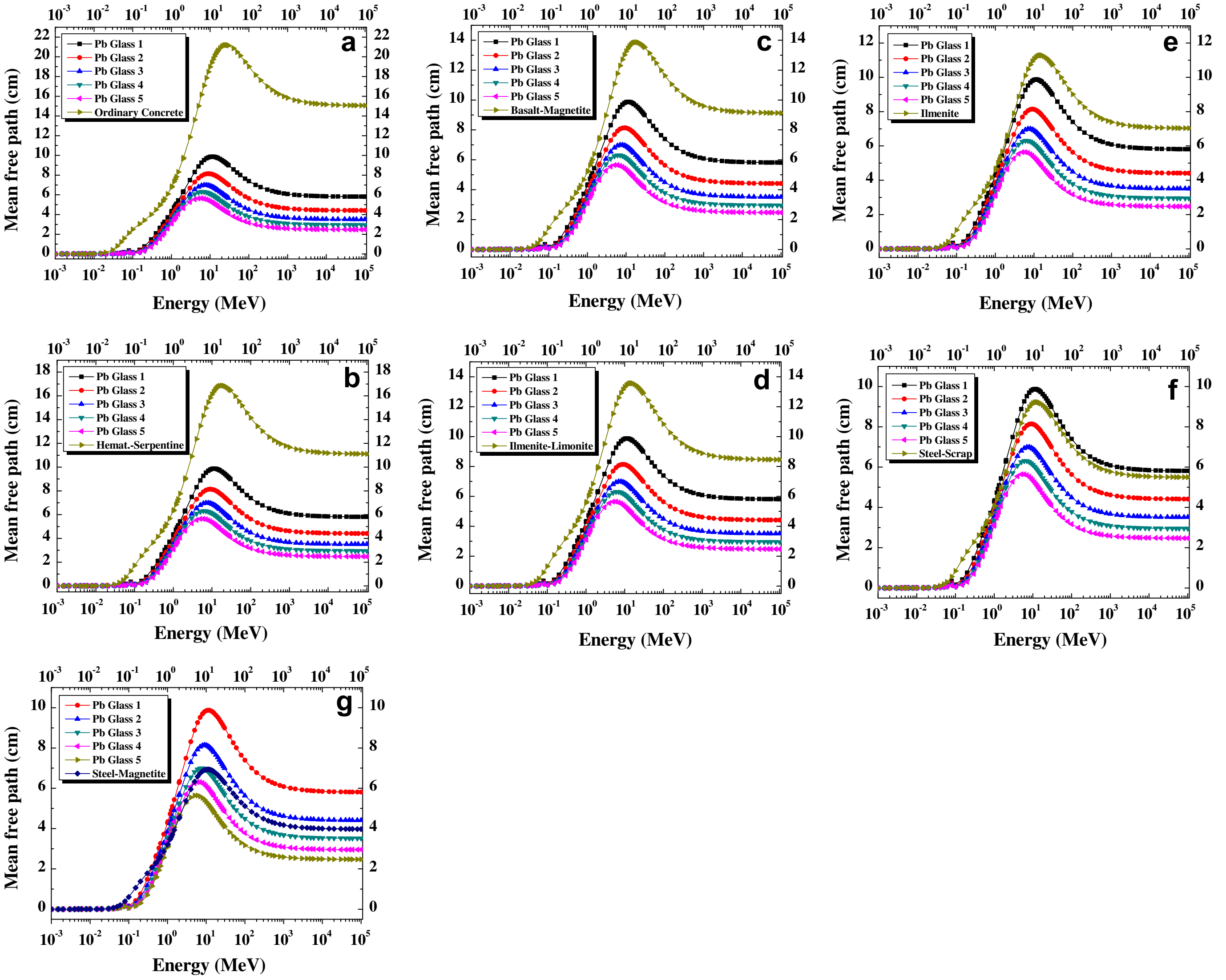

Fig. 5. (a–g) Mean free paths of PbO-B_2O_3 glass and different types of concretes in the energy region of 1 keV–100 GeV.

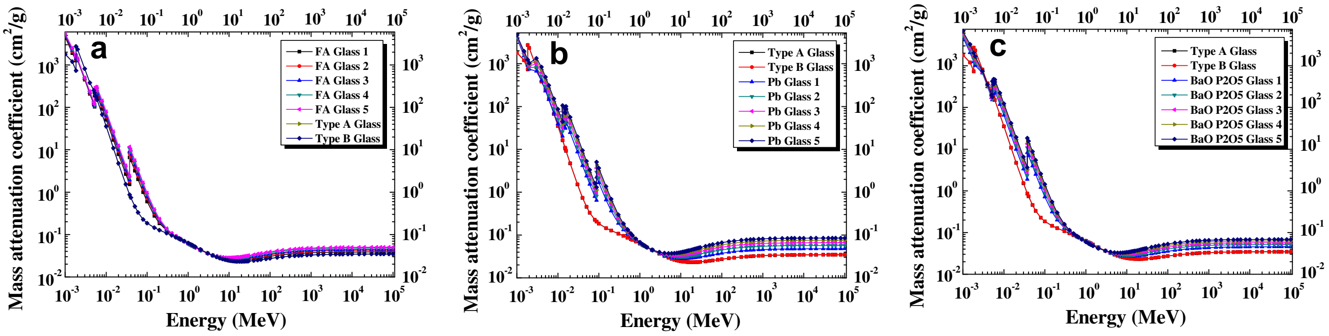

Fig. 6. (a–c) Total mass attenuation coefficients of heavy metal based glass systems and different types of commercial window glasses in the energy region of 1 keV–100 GeV.

4. Conclusions

From the results it can be concluded that the parameter Z_{eff} is energy dependent and takes values lower or higher depending on the partial photon interaction processes namely photoelectric absorption, Compton scattering and pair production. Below 100 keV, Z_{eff} seems to be inappropriate for estimating shielding property due to the non-uniform variation of this parameter which arises from *K* edge effects. It has been also observed that the lead free glass systems have higher values of Z_{eff} when compared to lead based glasses at some high energy regions even if they have lower mean atomic numbers. When compared with some standard shielding concretes and commercial window glasses, most of the glass samples have lower values of mfp than concretes and the present glass systems have higher values of total mass attenuation coefficients than commercial window glasses, thus confirming the availability of using these glasses as substitutes for some shielding concretes and commercial window glasses to improve radiation-shielding properties in the continuous energy region (1 keV–100 GeV).

References

[1] S.R. Manohara, S.M. Hanagodimath, L. Gerward, J. Nucl. Mater. 393 (2009) 465–472.
[2] M. Kurudirek, M. Aygun, S.Z. Erzeneoğlu, Appl. Radiat. Isot. 68 (2010) 1006–1011.
[3] M. Kurudirek, M. Buyukyildiz, Y. Özdemir, Nucl. Instrum. Methods A 613 (2010) 251–256.
[4] G.J. Hine, Phys. Rev. 85 (1952) 725.
[5] S. Singh, A. Kumar, D. Singh, S.K. Thind, G.S. Mudahar, Nucl. Instrum. Methods B 266 (2008) 140–146.
[6] K. Kirdsiri, J. Kaewkhao, A. Pokaipisit, W. Chewpraditkul, P. Limsuwan, Ann. Nucl. Energy 36 (2009) 1360–1365.
[7] J. Kaewkhao, P. Limsuwan, Nucl. Instrum. Methods A 619 (2010) 295–297.
[8] J. Kaewkhao, A. Pokaipisit, P. Limsuwan, J. Nucl. Mater. 399 (2010) 38–40.
[9] K. Singh, H. Singh, V. Sharma, R. Nathuram, A. Khanna, R. Kumar, S.S. Bhatti, H.S. Sahota, Nucl. Instrum. Methods B 194 (2002) 1–6.
[10] R.A. Rahimi, G. Raisali, S.K. Sadrnezhaad, A. Alipour, J. Nucl. Mater. 385 (2009) 527–532.
[11] S.R. Manohara, S.M. Hanagodimath, K.S. Thind, L. Gerward, Nucl. Instrum. Methods B 266 (2008) 3906–3912.
[12] L. Gerward, N. Guilbert, K.B. Jensen, H. Levring, Radiat. Phys. Chem. 60 (2001) 23–24.
[13] L. Gerward, N. Guilbert, K.B. Jensen, H. Levring, Radiat. Phys. Chem. 71 (2004) 653–654.
[14] M. Kurudirek, I. Türkmen, Y. Özdemir, Radiat. Phys. Chem. 78 (2009) 751–759.
[15] I.I. Bashter, Ann. Nucl. Energy 24 (1997) 1389–1401.
[16] P. Fuochi, U. Corda, M. Lavalle, A. Kovàcs, M. Baranyai, A. Mejri, K. Farah, Nukleonika 54 (2009) 39–43.